

Journal Pre-proof

Bertalanffy-Pütter models for the first wave of the COVID-19 outbreak

Norbert Brunner, Manfred Kühleitner

PII: S2468-0427(21)00024-5

DOI: <https://doi.org/10.1016/j.idm.2021.03.003>

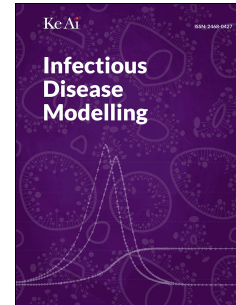
Reference: IDM 213

To appear in: *Infectious Disease Modelling*

Received Date: 28 October 2020

Revised Date: 8 March 2021

Accepted Date: 8 March 2021



Please cite this article as: Brunner N. & Kühleitner M., Bertalanffy-Pütter models for the first wave of the COVID-19 outbreak, *Infectious Disease Modelling* (2021), doi: <https://doi.org/10.1016/j.idm.2021.03.003>.

This is a PDF file of an article that has undergone enhancements after acceptance, such as the addition of a cover page and metadata, and formatting for readability, but it is not yet the definitive version of record. This version will undergo additional copyediting, typesetting and review before it is published in its final form, but we are providing this version to give early visibility of the article. Please note that, during the production process, errors may be discovered which could affect the content, and all legal disclaimers that apply to the journal pertain.

© 2021 The Authors. Publishing services by Elsevier B.V. on behalf of KeAi Communications Co. Ltd.

Title: Bertalanffy-Pütter models for the first wave of the COVID-19 outbreak

Short Titel: Bertalanffy-Pütter models for COVID-19

Authors: Norbert Brunner and Manfred Kühleitner¹

E-mail of all authors:

norbert.brunner@boku.ac.at, manfred.kuehleitner@boku.ac.at

Affiliation of all authors:

University of Natural Resources and Life Sciences (BOKU),
Department of Integrative Biology and Biodiversity Research (DIBB),
A-1180 Vienna, Austria

Corresponding author: Manfred Kühleitner

Institute of Mathematics, DIBB, BOKU
Gregor Mendel Strasse 33, A-1180 Vienna, Austria

E-Mail: manfred.kuehleitner@boku.ac.at

¹ Corresponding author: manfred.kuehleitner@boku.ac.at

Bertalanffy-Pütter models for the first wave of the COVID-19 outbreak

1

2

ABSTRACT: The COVID-19 pandemic challenges governments across the world. To develop adequate responses, they need accurate models for the spread of the disease. Using least squares, we fitted Bertalanffy-Pütter (BP) trend curves to data about the first wave of the COVID-19 pandemic of 2020 from 49 countries and provinces where the peak of the first wave had been passed. BP-models achieved excellent fits (R-squared above 99%) to all data. Using them to smoothen the data, in the median one could forecast that the final count (asymptotic limit) of infections and fatalities would be 2.48 times (95% confidence limits 2.42-2.6) and 2.67 times (2.39-2.765) the total count at the respective peak (inflection point). By comparison, using logistic growth would evaluate this ratio as 2.00 for all data. The case fatality rate, defined as the quotient of the asymptotic limits of fatalities and confirmed infections, was in the median 4.85% (confidence limits 4.4%-6.5%). Our result supports the strategies of governments that kept the epidemic peak low, as then in the median fewer infections and fewer fatalities could be expected.

16

Key Words: Akaike information criterion (AIC), Bertalanffy-Pütter model (BP-model), COVID-19 pandemic, epidemic trajectory, least-squares method, simulated annealing algorithm

19

20 **1. Introduction**

21 *1.1. Modeling approaches*

22 The first wave of the novel COVID-19 disease has challenged governments across the world.
23 Most states reacted swiftly, closing borders, and imposing stay-at-home rules. Within a few
24 weeks they could curb the further spread of the coronavirus SARS-CoV2, but the economic
25 costs were high. In the meantime, new waves emerged, and we ask: What lessons could be
26 drawn from the first wave?

27 This paper focuses on epidemic modeling using trend analysis, but with a goal that differs
28 from the common applications of this method. Rather than using trend-lines for the
29 forecasting of epidemic trajectories we used them to smoothen the data, because the data
30 might have been blurred by random fluctuations and errors (e.g. delays in reporting). The
31 smooth curves were then used to derive certain statistics for the time-series of infections.

32 Trend analysis was already applied successfully for the modeling of COVID-19. For example,
33 exponential (Malthusian) growth has been used to describe the initial explosive spread of
34 infections (Remuzzi & Remuzzi 2020). However, exponential growth is not suitable for the
35 modeling of data with a peak. Such data need models with sigmoidal (S-shaped) growth
36 curves. For this purpose, the Verhulst (1838) model of logistic growth has been particularly
37 popular (Google scholar: about 250 papers per month about “COVID-19” and “logistic
38 growth”). Logistic growth has achieved good fits to data from China (Shen 2020) and Italy
39 (Vattay 2020), but for other data the fit has not been that good (Kamrujjaman et al. 2020).

40 A major drawback of the logistic model is the inflexibility with respect to the inflection point:
41 At the peak of the outbreak (inflection point) the logistic model predicts a doubling of the
42 current cumulated count as the final size of the disease (asymptotic size). Thus, logistic
43 growth was not suitable for the study of the ratio of asymptotic size over peak size, because

44 for logistic growth this ratio is fixed independently of the actual data and the actual policy
 45 responses. (A similar argument applies to many more growth models, e.g. Brody or
 46 Gompertz.) Realistic forecasts for this ratio can only be expected from models that are more
 47 flexible with respect to the relation between the inflection point (peak) and the asymptotic
 48 limit (final size).

49 We therefore use the Bertalanffy-Pütter (BP) model to describe the growth of COVID-19. Its
 50 growth curves are solutions of differential equation (1). The model was introduced by Pütter
 51 (1920). Bertalanffy (1957) popularized it for modeling animal growth and recently Chowell
 52 (2017) introduced it into epidemiology under the name “generalized Richards model”. It was
 53 recently used to describe the first wave of COVID-19 in China (Wu et al. 2020).

$$(1) \quad y'(t) = p \cdot y(t)^a - q \cdot y(t)^b$$

54 Equation (1) describes cumulative case-counts by a function $y(t)$ of time (t in days). Thereby,
 55 $t = 0$ represents the first data-point and the five free model parameters are the non-negative
 56 exponent-pair $a < b$ (logistic growth: $a = 1$, $b = 2$), non-negative scaling constants p and q ,
 57 and the initial value $y(0) = c > 0$. (“Free” means that the parameters are determined from
 58 fitting the model to the data.)

59 ***1.2. Problem of the paper***

60 First, we explored the goodness of fit of the five-parameter BP-model (1) to COVID-19 data.
 61 We selected a sample of 49 countries and provinces, whose data for the first wave displayed a
 62 peak, i.e. during the first wave the countries had succeeded in “flattening the curve”. Using
 63 the method of least squares, for each country/province we fitted BP-models to two time-
 64 series, cumulated counts of fatalities and of confirmed cases (diagnosed infections).

65 Second, for each country and time-series (confirmed cases, fatalities) we used the BP-models
66 to compute certain statistics of practical significance and study them with statistical methods,
67 such as the asymptotic limits (final sizes of the first wave), the inflection points (peaks of the
68 first wave) and statistics computed from them, specifically final size over peak size. Given the
69 sample of 49 countries/provinces, which value of this ratio was typical for the first wave of
70 COVID-19? Could we distinguish between countries that had a good or a poor performance
71 during the first wave of COVID-19?

72 Third, to explore the utility of BP-models for forecasting, we fitted it to the initial half of the
73 data and compared its extrapolation with the actual epidemic trajectories. For this purpose, we
74 considered a calibration by means of weighted least squares using a new weighing scheme.

75 **2. Method**

76 **2.1. Data**

77 We retrieved the data for this paper from CSSE (2020). This source collects for various
78 entities (countries and provinces) the daily counts of confirmed infections, of deaths and of
79 recovered patients, and it updates this information daily. However, for several countries the
80 source does not record the count of recovered patients, whence for this paper for each of 49
81 countries and provinces we used two time-series, fatalities and confirmed cases. To ensure
82 reproducibility of our data, we defined a reference day (June 18, 2020), so that each time-
83 series started at the first nonzero entry for that country/province (indicator cases and first
84 fatalities, respectively) and it terminated on the reference day (Table 1). The resulting time-
85 series reported daily counts for 47-148 days.

86 The time-series for the confirmed infections in the Chinese province of Hubei was insofar
87 exceptional, as it started with 444 confirmed cases. (As the pandemic started in Hubei and the
88 disease was unknown then, the earlier counts were obtained with different methods and the

89 source had removed the initial segment of this time-series; the same for the fatalities.) Further,
90 the data for the USA pertain mainly to the first wave in the Northeast, where a “flattening of
91 the curve” was discernable, although the first wave in the other states just has begun.

92 For the choice of our sample of countries, we selected only countries/provinces that had
93 succeeded in the flattening of the growth curve prior to the reference day. (Thus, the epidemic
94 peak and the final size could be discerned roughly.) We used this criterion because our
95 research question relates the peak to the final size. Further, we wished to utilize the
96 observation that BP-type would be particularly suitable for the modeling of data that include
97 the after-peak stage (Sornette et al., 2020).

98 Moreover, we aimed at a sample that represents all parts of the world, including extremely
99 poor and rich countries (e.g. Burkina Faso and Norway). Also the demographic structure of
100 the countries differed (the case fatality rate is known to increase with age), as did their
101 medical infrastructures (e.g. access to intense care units), and the transmission patterns (e.g.,
102 ethnic and socio-economic factors, social interactions and clusters may matter). Consequently,
103 for the countries of our sample the reactions to and experiences with COVID-19 varied
104 widely, from a lockdown in the Chinese province of Hubei to mere appeals for more personal
105 responsibility in Sweden, from intense care units that remained below their capacity in
106 Austria to a breakdown of the public health system in Italy.

107 As official COVID-19 data may be distorted for political reasons, we used an independent and
108 well-esteemed source (CSSE 2020). However, there remained a problem of underreporting, as
109 a peculiarity of COVID-19 is the large number of asymptomatic carriers. According to one
110 source (Ferretti et al. 2020), up to 50% of COVID-19 infections may happen from carriers
111 that have not developed symptoms yet. Further, the pre-symptomatic incubation period is
112 relatively long (WHO 2020.) Thus, to detect and insulate infected persons depends largely on
113 the intensity of testing, which in turn may vary considerably over time (e.g. initial shortage of

114 test kits) and between countries. (Thus, in China 86% of infections may have remained
 115 undetected prior to the lockdown of Wuhan: Li et al. 2020.) To reduce this type of inevitable
 116 data uncertainty, we used two time-series per country in parallel, death tolls in addition to the
 117 counts of confirmed infections, as we did not expect a significant number of undetected
 118 COVID-19 deaths. However, the two trajectories did not develop perfectly in parallel, as the
 119 case fatality rate increased significantly, when in some countries the public health systems
 120 were overcharged (Vattay 2020).

121 **2.2. Calibration and model selection**

122 We used the (ordinary) least-squares method, which is the most common tool of calibration,
 123 and variants of it. It measures the goodness of the fit to the data by means of *SSE*, the sum of
 124 squared errors (fit residuals) in equation (2). We sought five parameters (a, b, c, p, q), so that
 125 for the solution $y(t)$ of equation (1) the following sum *SSE* was minimized, whereby y_i was the
 126 total count up to time t_i and n was the length of the time-series of data-points:

$$(2) \quad SSE = \sum_{i=1}^n (y_i - y(t_i))^2$$

127 In the context of forecasting we developed an alternative measure for the goodness of fit,
 128 weighted least-squares that aimed at finding parameters to minimize the following sum (3) of
 129 weighted squared errors *SWSE*:

$$(3) \quad SWSE = \sum_{i=1}^n \frac{(y_i - y(t_i))^2}{|y'(t_i)|}$$

130 Another measure for the goodness of fit related to *SSE* is the coefficient of determination, R-
 131 squared (R^2) of equation (4). It compares the model-fit with the fit by the trivial constant
 132 model (relative improvement) and can be used to assess the goodness of fit across different
 133 datasets.

$$(4) \quad R^2 = 1 - \frac{SSE}{\sum_{k=1}^n (y_k - \text{mean}(y_1, y_2, \dots, y_n))^2}$$

134 In view of certain limitations for the interpretation of R-squared, in this paper we did not use
 135 it for model-selection. For such a purpose the Akaike information criterion (*AIC*), equation
 136 (5), was shown to be more selective (Spiess & Neumeyer 2010). We therefore used *AIC* for
 137 model comparison and used R-squared merely to inform about the goodness of fit by means
 138 of a well-known statistic.

$$(5) \quad AIC = n \cdot \ln\left(\frac{SSE}{n}\right) + 2 \cdot K$$

139 Here, n is the number of data-points and K is the number of optimized parameters of the
 140 model. ($K = 6$ for the general BP-model, counting a, b, c, p, q and SSE , and $K = 4$ for logistic
 141 growth, where $a = 1, b = 2$ are not optimized.) When comparing two models, the model with
 142 the lower *AIC* is selected (Burnham & Anderson 2002, Motulsky & Christopoulos 2003),
 143 whereby *AIC* penalizes the model with more parameters. When comparing a model with the
 144 best-fit model (*AIC* and AIC_{min} , respectively), then equation (6) computes the probability, \wp ,
 145 that the (worse) model with higher *AIC* would be “true”, when compared to the model with
 146 the least *AIC* (Burnham & Anderson 2004). Note that a difference of *AIC* above 10 strongly
 147 supports the refutation of the model with a higher *AIC* ($\wp < 0.7\%$).

$$(6) \quad \wp = \frac{\exp\left(-\frac{AIC - AIC_{min}}{2}\right)}{1 + \exp\left(-\frac{AIC - AIC_{min}}{2}\right)}$$

148 **2.3. BP-model and optimization**

149 The BP-model generalizes several well-known models. Special cases are the Brody (1945)
 150 model of bounded exponential growth with exponent-pair $(a, b) = (0, 1)$, Verhulst (1838)
 151 logistic growth with pair $(1, 2)$, or the model of von Bertalanffy (1957) with $(2/3, 1)$. The

152 Gompertz (1832) model fits into this scheme, too: It is the limit case of the pair (1, 1), but
 153 with a different differential equation (Marusic & Bajzer 1993). Equation (1) also includes
 154 several models with four free parameters, such as the generalized Bertalanffy model ($b = 1$
 155 with $0 \leq a < 1$ variable), the Richards (1959) model ($a = 1$ with $b > 1$ variable), or the
 156 generalized logistic model ($b = a+1$ with $a > 0$ variable; c.f. Roosa et al. 2020).

157 For the BP-model, the relation between the asymptotic limit (size) y_{max} and the inflection
 158 point at time t_{infl} with size y_{infl} is given by equations (7) and (8). Thereby, the asymptotic limit
 159 estimates the final size of (the first wave of) the disease; the inflection point represents the
 160 peak of (the first wave of) the epidemics. If $q = 0$, then the growth function is unbounded, and
 161 if $a = 0$, then there is no inflection point.

$$(7) \quad y_{max} = \left(\frac{p}{q}\right)^{\frac{1}{b-a}} \quad \text{if } q > 0$$

$$(8) \quad y_{infl} = \left(\frac{a}{b}\right)^{\frac{1}{b-a}} \cdot y_{max} \quad \text{if } a > 0 \text{ and } q > 0$$

162 As follows from equation (8), for logistic growth the ratio y_{max}/y_{infl} is fixed (ratio = 2, because
 163 $a = 1, b = 2$), whereas for model (1) with variable exponent-pairs any ratio larger than 1 can
 164 be attained. Further, model (1) always fits better to the data than the logistic growth model, as
 165 it generalizes this model. (The same for any other three-parameter BP-model with given
 166 exponent-pair.)

167 For certain BP-models with three or four parameters, there are different parametrizations that
 168 aim at describing model (1) in terms of growth parameters that are meaningful for animals
 169 (c.f. Tjørve & Tjørve 2017). For the general five-exponent BP-model, such parametrizations
 170 are not available, as although equation (1) can be solved analytically, non-elementary
 171 functions are needed for the solution of the general equation (Ohnishi et al. 2014).

172 Standard optimization tools did not always identify the best-fit parameters for the five-
173 parameter BP-model. We therefore used a custom-made optimization method using the
174 Mathematica code from Renner-Martin et al. (2018). The method searches the best-fit
175 exponent-pair on a given search-grid (which is adapted during optimization) and for each
176 fixed grid-point exponent-pair (a, b) it uses a variant of simulated annealing to identify the
177 best-fitting remaining parameters (c, p, q) . Simulated annealing (Vidal 1993) uses elements of
178 a random search to escape a suboptimal local minimum, which is an advantage in the
179 presence of many local optima (as for the present optimization problem). This approach
180 identified BP-model parameters with growth curves close to the data.

181 **2.4. Statistical analysis**

182 For each dataset, we used the best-fit BP-model to compute various statistics. For example,
183 the ratios y_{max}/y_{infl} for the time series of fatalities defined a random sample (of size 49) and we
184 then used standard methods from statistics to further analyze this sample. Note that our paper
185 aimed at a comparison of countries in terms of these COVID-19 statistics, following the
186 example of literature in comparative international law (e.g. Hathaway 2002; Magesan 2013;
187 Brunner & Tschohl 2014). Therefore, we were not interested in the variability of a statistic for
188 a single time-series, but we studied the variability of a statistic across different the time-series
189 for different countries.

190 In view of the unknown distributions and the small sample size, we used primarily non-
191 parametric methods, e.g. Spearman rank test for correlations, Siegel-Tukey-test for the
192 variance, sign-test for location parameters. (The true distributions of our statistics were most
193 likely complicated; c.f. ratio-distributions in Díaz-Francés & Rubio 2013.)

194 In this paper, all confidence intervals assume 95% confidence. When we used nonparametric
195 tests to establish confidence intervals, we also informed about the actual (higher) level of

196 confidence. For instance, when we used the one-sided sign test for the confidence interval of a
197 median (Hollander & Wolfe 1999), we informed about the P-values of the lower and upper
198 confidence limits, as in view of the discrete nature of the test these were not always equal.

199 For some statistics we were interested in their distributions. Thereby, we used the Anderson-
200 Darling-test to check certain simple assumptions for continuous distributions. (For
201 distributions different from the normal distribution we applied this test using 5000 Monte-
202 Carlo simulations.) For a P-value below 5% we refuted the distribution assumption. To check,
203 if the underlying distribution of samples A and B differed, we tested, if sample A was
204 distributed according to the smooth kernel distribution of sample B.

205 **3. Results and discussion**

206 ***3.1. R-squared of the best-fit BP-model curves***

207 Table 2 and Table 3 lists the best-fit parameters of the BP-model and inform about the
208 goodness of fit: Note that other than suggested by Chowell (2017), optimization needed
209 exponents $a > 1$. For the 49 time-series of fatalities, R-squared ranged between 99.06% and
210 99.98% and for the time-series of confirmed cases R-squared ranged between 98.46% and
211 99.97%. R-squared could be interpreted as a statistic associated to each time-series. Under
212 this viewpoint, the median of the pooled R-squared values (i.e. 98 values) was 99.83%. The
213 lower and upper confidence limits for the median were 99.785% and 99.865%. (For each of
214 these limits a one-sided sign-test for the hypothesis that this limit would be a median resulted
215 in the P-value 1.668%, whence the actual confidence level was 96.7%.)

216 For logistic growth, the fit was excellent, too, with the 98 R-squared values in the range
217 between 96.50% and 99.93%. While the R-squared values for logistic growth were smaller,
218 but still comparable to those of the best-fit BP-model, the Akaike information criterion
219 indicated that logistic growth was false in comparison to the best-fit BP-model, except for one

220 time-series (Canada, Alberta, cumulated confirmed cases). For 92 of the 98 time series,
221 logistic growth was most likely false (*AIC* difference of 10 or higher).

222 The good fit of the general BP-model to all data confirmed the utility of our custom-made
223 approach of grid-optimization, while well-established optimization tools failed to converge.
224 An example for such a failure relates to the Levenberg-Marquart (LM) algorithm that was
225 employed by Wu et al. (2020): In terms of R-squared, the supporting information of that paper
226 reported for Shanghai $R^2 = 86.7\%$ for the five-parameter BP-model, while for logistic growth
227 they reported the better fit $R^2 = 88.1\%$. Thus, the LM-algorithm failed to find the optimal
228 model parameters for the five-parameter BP-model, because the general model necessarily
229 should achieve a better fit than its special case of logistic growth.

230 Finally, we note that we fitted the model curve to the cumulated data and not to the daily new
231 cases, which display much more random fluctuation and therefore results in a lower R-
232 squared. By data-fitting to daily cases we mean the fitting of the temporal derivative $m'(t)$ to
233 the daily data. In a different context we have shown that the growth curve $m(t)$ with the best
234 fit to the cumulated data may be suitable to model the daily data, too, if a time-shift t_s is added
235 (Ziegler et al. 2020). The reason, why some authors prefer fitting $m'(t)$ to daily data rather
236 than fitting $m(t)$ to cumulated data is the possible underestimation of the size of the
237 confidence intervals for the parameters (Shen 2020). This problem does not matter for this
238 paper, as we focus on comparisons of countries.

239 As for a limitation, note that the grid-optimization of this paper was not suitable to compute
240 confidence intervals for the best-fit BP-model parameters to a particular time-series. The
241 reason is the CPU-time needed for optimization: To estimate confidence intervals, the
242 optimization would have to be repeated for several hundred random perturbations of the data.
243 However, for the problem of this paper such confidence bounds were not needed, as we used
244 the best-fit model merely to smoothen the data by means of a sigmoidal growth function and

245 compute the inflection point. Thereby, we were not interested in the variability of the
246 inflection point with respect to a specific time-series (confidence bounds), because we
247 compared the inflection points from different time-series of different countries, where we
248 expected a much higher variability.

249 *3.2. Asymptotic limits and forecasting from subsamples*

250 Figure 1 illustrates a difficulty in estimating the final size of the first wave. The cumulated
251 counts of fatalities in Austria (blue dots) continued to increase slowly, as the epidemics did
252 not end with the first wave. (Specifically, there was a jump at $t = 76$ from 645 to 668
253 fatalities.) Therefore, there was no clear-cut definition of the “end of the first wave” and of its
254 final size. We explored this issue by comparing for two calibrations (*SSE* and *SWSE*) the BP-
255 model growth curves fitted to the full data (96 data-points) and the one fitted to the initial half
256 of the data (48 data-points). For *SSE*, the growth curves fitted well to the first 55 data-points
257 and to the data-points after the jump. Thereby the curve fitted to the initial 48 data-points (red
258 solid line) had a slightly lower asymptotic limit than the one fitted to the full data (black solid
259 line). This observation generalizes, as for *SSE* the asymptotic limit computed for an initial
260 segment of the data in general underestimates the final size (Kühleitner et al. 2019). Thus,
261 *SSE* could be used if all data-points came from the first wave. The growth curve for *SWSE*
262 that was fitted to the initial 48 data-points (dashed red line) appeared to fit best to the initial
263 76 data-points, but it fitted poorly to the data-points after the above-mentioned jump. Thus,
264 this growth curve could be used, if the first wave ended prior to the jump. The growth curve
265 for *SWSE* that was fitted to the full data (dashed black line) appeared to fit worst, whereby the
266 weights for *SWSE* by design tolerate a higher variability in the total count during the epidemic
267 peak (where data uncertainty might be largest).

268 In view of the similar behavior of the two growth curves for *SSE* (solid lines) and the
269 problematic fit of the latter *SWSE* growth curve, we decided to analyze the country
270 performances by fitting a BP-growth curve to the full data and use *SSE* for calibration.

271 In the following sense this decision led us to implicitly assume that for our data the first wave
272 lasted till the reference day (June 18) or ended only shortly before it. For, in the median over
273 the considered time-series the cumulated counts on the reference day (Table 1), i.e. the
274 maximal count $\max(y_i)$, differed barely from the asymptotic limits y_{max} of the BP-model
275 curves that were fitted to the 98 time-series (Table 4). Thereby, equation (7) was used to
276 compute y_{max} and we used the quotients $y_{max}/\max(y_i)$ as a test-statistic (Table 5). For the
277 combined sample of 98 quotients, the median of the quotients was 0.994, whereby the lower
278 and upper confidence limits were 0.9865 and 1. (The P-values of one-sided sign-tests were
279 1.668% and 2.72%, respectively, amounting to 95.6% confidence.) Thus, in the median the
280 quotients were close to one, but slightly smaller. (This was to be expected, as the epidemics
281 continued after the first wave.)

282 Notably, the different types of time-series differed with respect to the quotients $y_{max}/\max(y_i)$:
283 The variance of the two samples of 49 quotients, one for fatalities and the other for confirmed
284 cases, differed significantly (Siegel-Tukey test: P-value close to 0). Indeed, 95% of the
285 quotients for the time-series of fatalities were in the interval between 0.954 and 1.131 (2.5%
286 and 97.5% quantiles), while the same interval for the confirmed cases had the endpoints 0.871
287 and 2.013.

288 **3.3. Forecasting the final size from the peak**

289 We utilized the good approximation of the data by BP-growth functions (calibration: *SSE*) to
290 obtain estimates for the peak y_{infl} (inflection point) from equation (8). Next, when comparing
291 the final size and the peak size of the first wave of the epidemics we could ask: What forecast

292 about the final size could be drawn at the peak, i.e.: how many further victims were to be
293 expected once the peak had been reached? Thereby, countries that had comparably low peak
294 counts (y_{infl}) had comparably low final counts at the end of the first wave (asymptotic limit
295 y_{max}). While for both types of data (confirmed cases, fatalities) the correlation between peak
296 size and final size was high (Spearman rho close to 1) and highly significant (Spearman rank
297 test for independence: P-values close to 0), this correlation was associated to country size. To
298 eliminate this dependency, we studied the ratios y_{max}/y_{infl} for the 98 time-series (Table 5).

299 Figure 2 illustrates the use of the BP-model for this problem by the example of Burkina Faso:
300 The blue dots represent the reported fatalities. To smoothen the data, we identified the best-fit
301 trajectory of the best fitting BP-model (black curve). We then used this model curve to
302 estimate the epidemic peak (red: inflection point) and the final size (red line: asymptotic
303 limit). While the fit by the logistic growth curve (green) to the data was clearly poorer, its
304 asymptotic limit did not differ significantly from that of the best-fit growth curve. However,
305 the drawback of the logistic growth curve was its data-independent ratio $y_{max}/y_{infl} = 2$
306 (resulting in a clearly distinct estimate for the inflection point, see red dots in Figure 2). Using
307 the best-fit BP-model the ratio for final size over peak size was $y_{max}/y_{infl} = 2.6$.

308 For all 49 time-series of cumulated counts of confirmed infections, the best-fit BP-model had
309 an inflection point and the ratios y_{max}/y_{infl} ranged from 1.7 to 16. The median of y_{max}/y_{infl} was
310 2.48 with lower and upper confidence limits 2.42 and 2.6 (one-sided sign-tests: P-value 2.2%
311 for both limits and therefore confidence level 95.6%). For the cumulated counts of fatalities,
312 the best-fit BP-model to the time-series of Uruguay was without inflection point. For the
313 remaining 48 time-series, the ratios y_{max}/y_{infl} ranged from 1.42 to 4.12. The median of y_{max}/y_{infl}
314 was 2.67 with lower and upper confidence limits 2.39 and 2.765 (one-sided sign-tests: P-
315 values 2.97% and 1.47% for the lower and upper limit, respectively, and therefore confidence
316 level 95.6%).

317 We note that the ratios y_{max}/y_{infl} were (stochastically) higher for the time-series of fatalities:
 318 Removing Uruguay temporarily from the dataset (no inflection point), 2/3 of the 48 remaining
 319 countries/provinces (i.e.: all, except nine) had a higher ratio y_{max}/y_{infl} for the fatalities than for
 320 the confirmed infections (one-sided sign-test: P-value 1.5%). Further, the ratios for the
 321 fatalities and confirmed infections were correlated (Spearman rho 0.332 with P-value 2.1%
 322 for the Spearman rank test of independence).

323 The distributions of the ratios y_{max}/y_{infl} differed between the samples of confirmed cases and
 324 fatalities (Anderson-Darling test for equal distributions: P-value 0.9%, using a smooth kernel
 325 distribution). However, two different Cauchy-distributions could be fitted to the samples
 326 (Anderson-Darling test: P-value 26.6% for the fatalities and 56.6% for the confirmed
 327 infections). Recall that the Cauchy distribution has the cumulative distribution function
 328 $CDF(x) = 0.5 + \arctan((x-m)/s)/\pi$. Using the maximum-likelihood parameters ($m = 2.6209$,
 329 $s = 0.272202$ for fatalities, $m = 2.4828$, $s = 0.154565$ for confirmed cases) we obtained the
 330 confidence intervals $[1, 6.08]$, and $[1, 4.447]$ for the ratios for fatalities and confirmed
 331 infections, respectively. (The upper limits are the 97.5% quantiles of the distributions. For the
 332 lower limits, always $y_{max}/y_{infl} \geq 1$. Note that compared to the cumulative histogram, CDF
 333 overestimated the probability of ratios below 2.)

334 **3.4. Case fatality rates**

335 The case fatality rate of a disease in a country is the number of dead over the number of
 336 diagnosed infections at a certain moment of time. When used for estimating the plausible
 337 lethality (*IFR*: infection fatality rate), there is a bias, as the count of recovered persons is not
 338 considered (Ghani et al. 2005) and as a correction for the time-lag between becoming infected
 339 and dying is needed (Russell et al. 2020). Further, for COVID-19 there is an additional
 340 uncertainty in view of the unknown number of asymptomatic infections that never have been
 341 identified. For this reason we considered a time-independent asymptotic version for the first

342 wave of COVID-19 and we used it for country comparison (rather than for estimating *IFR*):
343 *CFR* is the asymptotic limit of fatalities over the asymptotic limit of confirmed cases
344 (Table 5).

345 *CFR* varied widely between the countries, from 0.5% for the United Arab Emirates to 16.2%
346 for Belgium. The seven countries with the largest *CFR*-values were Spain (*CFR* = 11.7%),
347 Netherlands (12.7%), United Kingdom (13.8%), Hungary (14%), Italy (14.7%), France
348 (15.7%), and Belgium (16.2%).

349 The median *CFR* was 4.85% and the limits of the confidence interval for the median were
350 4.4% and 6.5%. (Using a one-sided sign-test the P-value was 2.22% for each limit, resulting
351 in a confidence level of 95.6%.) Was the variability of *CFR* compatible with the hypothesis of
352 random fluctuations? In other words, did a *CFR* above/below the median indicate a poor/good
353 policy response? We observed that even the high *CFR*-values were within the range of
354 statistical fluctuations of a lognormal distribution. Thereby first, for the full sample of 49
355 *CFR*-values the hypothesis that their logarithms were normally distributed was not refuted by
356 the Anderson-Darling test (P-value 23.8%.) Second, assuming a lognormal distribution for
357 *CFR*, we used the maximum likelihood-method to identify its location and shape parameters
358 (-3.04606 and 0.731759 , respectively; median 4.7546%). This resulted in the 95%-confidence
359 interval for the *CFR*-values between 1.13% and 19.95%. The latter bound was higher than the
360 highest observed *CFR*.

361 **4. Conclusion**

362 We have compared the experiences of different countries with the first wave of COVID-19, as
363 this may help in shaping future responses.

364 As to our primary aim, we have shown that the general BP-model had excellent fits to the
365 epidemiological data of the considered countries (Section 3.1). It clearly outperformed logistic

366 growth. Based on 98 COVID-19 time-series the general BP-model achieved in the median
367 $R^2 = 99.83\%$ with a narrow 95% confidence interval. As a caveat, we claim this good fit only
368 for the problem of fitting the general BP-model to epidemic data that are cumulative and that
369 include the after-peak stage. For our data, the latter condition was confirmed by the statistic
370 “asymptotic limit over final count” (Section 3.2), whose median was close to one.

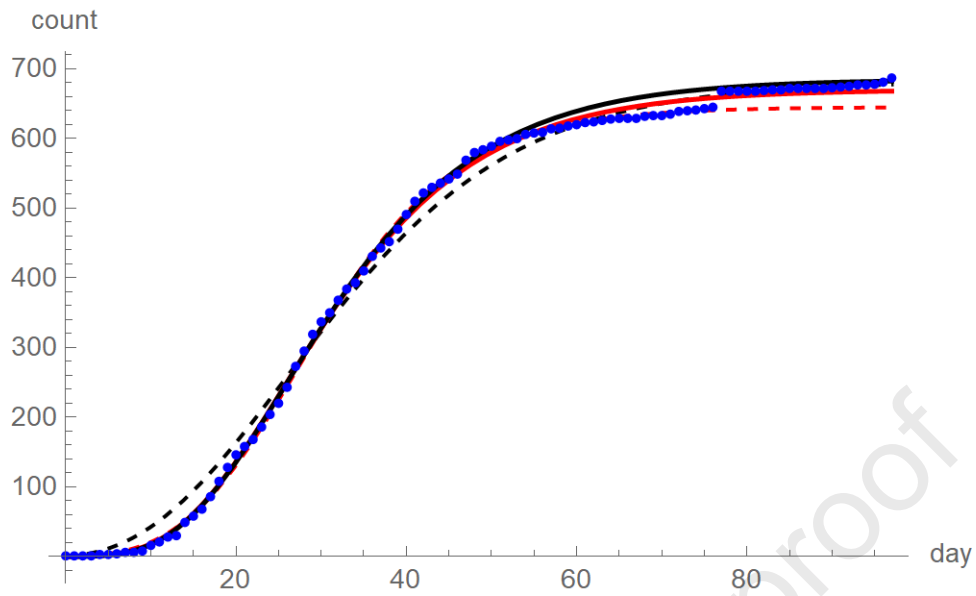
371 As to policy recommendations we found that countries that could keep the peak of the wave
372 low succeeded also in keeping the final size low (Section 3.3). We confirmed this by
373 modeling final size over peak size by the statistics “asymptotic limit over size at the inflection
374 point”. For the general BP-model this ratio was flexible and therefore (other than for logistic
375 growth with a fixed ratio of 2) it could be estimated from the data. Thereby, our data would
376 have supported the following forecasts for a country/province during the first wave of the
377 COVID-19 epidemics: Using the medians, at the peak of the confirmed infections one could
378 forecast that the final count of infections at the end of the wave would be about 2.5 times the
379 present peak count. Further, at the peak of fatalities the forecast for the final count of fatalities
380 would be 2.7 times the present peak count. Note that these forecasts extrapolated from the
381 sample of 49 countries/provinces. As to limitations for such forecasts, we assumed that these
382 countries would be representative for the global situation.

383 The case fatality rate, *CFR*, is another statistic of concern for epidemiologists (Section 3.4).
384 Did a high *CFR* indicate a policy failure? The median *CFR* was about 5%, but for some
385 countries it exceeded 10%. While it might be true that in countries with excessive *CFR*
386 something might have gone wrong, our data were consistent with the hypothesis of a
387 lognormal distribution for which high *CFR*-values were not unlikely. Thus, our data did not
388 allow to single out countries with a particularly good or bad performance.

389 **5. References**

- 390 Bertalanffy L.v. (1957) Quantitative laws in metabolism and growth. *Quarterly Revues in Biology* **32**: 217-231.
- 391 Brody S. (1945) *Bioenergetics and Growth*. Hafner Publ. Comp., New York, NY, USA.
- 392 Brunner N., Tschohl C. (2014) Do Patterns of Treaty Ratifications Reveal Societal Preferences? Analysis of
393 Twelve Council of Europe Conventions. *Jusletter-IT*, special issue: Proceedings of IRIS, 14-20 February
394 2014, Salzburg, Austria, published online at the Link: www.weblaw.ch.
- 395 Burnham K.P., Anderson D.R. (2002) *Model Selection and Multi-Model Inference: A Practical Information-*
396 *Theoretic Approach*. Springer, Berlin.
- 397 Burnham K.P., Anderson D.R. (2004) Multi-model inference. Understanding AIC and BIC in model selection.
398 *Sociological Methods & Research* **33**: 261-304.
- 399 Chowell G. (2017) Fitting dynamic models to epidemic outbreaks with quantified uncertainty: A primer for
400 parameter uncertainty, identifiability, and forecasts. *Infectious Disease Modelling* **2**: 379-398.
- 401 CSSE (2020) *COVID-19 Data Repository by the Center for Systems Science and Engineering (CSSE)*, Johns
402 Hopkins University, Baltimore, USA. Link: <https://github.com/CSSEGISandData/COVID-19>, last visit
403 21.07.2020.
- 404 Díaz-Francés E., Rubio F.J. (2013) On the existence of a normal approximation to the distribution of the ratio of
405 two independent normal random variables. *Statistical Papers* **54**: 309-323.
- 406 Ferretti L., Wymant C., Kendall M., 1, Zhao L., Nurtay A., Abeler-Dörner L., Parker M., Bonsall D., Fraser C.
407 (2020) Quantifying SARS-CoV-2 transmission suggests epidemic control with digital contact tracing.
408 *Science* **368**, published online: DOI 10.1126/science.abb6936
- 409 Ghani A.C., Donnelly C.A., Cox D.R., Griffin J.T., Fraser C., Lam T.H., Ho L.M., Chan W.S., Anderson R.M.,
410 Hedley A.J., Leung G.M. (2005) Methods for Estimating the Case Fatality Ratio for a Novel, Emerging
411 Infectious Disease. *American Journal of Epidemiology* **162**: 479-486.
- 412 Gompertz B. (1832) On the nature of the function expressive of the law of human mortality, and on a new mode
413 of determining the value of life contingencies. *Philos. Trans. R. Soc. London* **123**: 513-585.
- 414 Hathaway O.A. (2002) Do Human Rights Treaties Make a Difference? *Yale Law Journal* **111**: 1935-2042.
- 415 Hollander M., A. Wolfe D.E. (1999) *Nonparametric Statistical Methods*, Wiley, Chichester, UK.
- 416 Kamrujjaman M., Shahriar M, Shafiqul I. (2020) Coronavirus Outbreak and the Mathematical Growth Map of
417 COVID-19. *Annual Research & Review in Biology* **35**: 72-78.
- 418 Kühleitner M., Brunner N., Nowak W.G., Renner-Martin K., Scheicher K. (2019) Best-fitting growth curves of
419 the von Bertalanffy-Pütter type. *Poultry Science* **98**: 3587-3592.
- 420 Li R., Pei S., Chen B., Song Y., Zhang T., Yang W., Shaman J. (2020) Substantial undocumented infection
421 facilitates the rapid dissemination of novel coronavirus (SARS-CoV-2) *Science* **368**: 489-493.
- 422 Lo C.F. (2012) The sum and difference of two lognormal random variables. *Journal of Applied Mathematics*,
423 published online: DOI 10.1155/2012/838397.
- 424 Magesan A. (2013) Human Rights Treaty Ratification of Aid Receiving Countries. *World Development* **45**: 175-
425 188.
- 426 Marusic M., Bajzer Z. (1993) Generalized two-parameter equations of growth. *Journal of Mathematical Analysis*
427 *and Applications* **179**, 446-462.
- 428 Motulsky H., Christopoulos A. (2003) *Fitting Models to Biological Data Using Linear and Nonlinear*
429 *Regression: A Practical Guide to Curve Fitting*. Oxford University Press, Oxford, U.K.

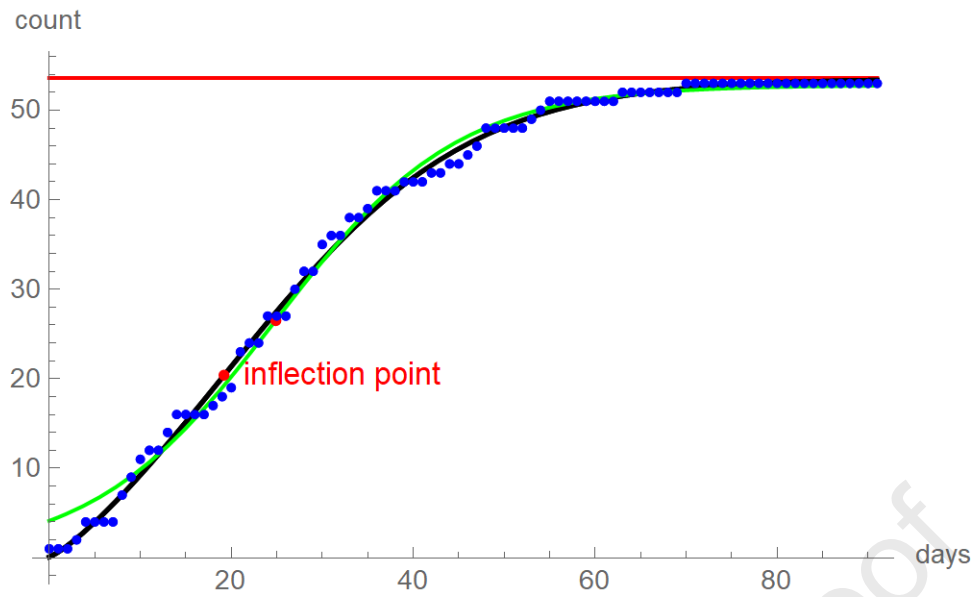
- 430 Ohnishi S., Yamakawa T., Akamine T. (2014) On the analytical solution for the Pütter-Bertalanffy growth
431 equation. *Journal of Theoretical Biology* **343**: 174-177.
- 432 Pütter A. (1920) Studien über physiologische Ähnlichkeit. VI. Wachstumsähnlichkeiten. *Pflügers Archiv für die*
433 *Gesamte Physiologie des Menschen und der Tiere* **180**: 298-340.
- 434 Remuzzi A., Remuzzi G. (2020) COVID-19 and Italy: what next? *The Lancet* **395**: 1225-1228.
- 435 Renner-Martin K., Brunner N., Kühleitner M., Nowak W.G., Scheicher K. (2018) Optimal and near-optimal
436 exponent-pairs for the Bertalanffy-Pütter growth model. *PeerJ* **6**, published online: DOI 10.7717/peerj.5973.
- 437 Richards F.J. (1959) A flexible growth function for empirical use. *Journal of Experimental Botany* **10**: 290-300.
- 438 Roosa K., Lee Y., Luo R., Kirpich A., Rothenberg R., Hyman J.M., Yan P., Chowell G. (2020) Short-Term
439 Forecasts of the COVID-19 Epidemic in Guangdong and Zhejiang, China: February 13–23, 2020. *Journal of*
440 *Clinical Medicine* **9**, published online: DOI 10.3390/jcm9020596.
- 441 Russell T.W., Hellewell J., Jarvis C.I., van Zandvoort K., Abbott S., Ratnayake R., Cmmid Covid-Working
442 Group, Flasche S., Eggo R.M., Edmunds W.J., Kucharski A.J. (2020) Estimating the infection and case
443 fatality ratio for coronavirus disease (COVID-19) using age-adjusted data from the outbreak on the Diamond
444 Princess cruise ship, February 2020. *Euro surveillance: European communicable disease bulletin* **25**,
445 published online: DOI 10.2807/1560-7917.ES.2020.25.12.2000256
- 446 Shen C.Y. (2020) Logistic growth modelling of COVID-19 proliferation in China and its international
447 implications. *International Journal of Infectious Diseases* **96**: 582-589.
- 448 Sornette D., Mearns E., Schatz M., Wu K., Darcet D. (2020) *Interpreting, Analyzing and Modelling COVID-19*
449 *Mortality Data*. Preprint published online: DOI 10.2139/ssrn.3586411.
- 450 Spiess A.N., Neumeyer N. (2010) An evaluation of R^2 as an inadequate measure for nonlinear models in
451 pharmacological and biochemical research: a Monte Carlo approach. *BMC Pharmacology* **10**, published
452 online: DOI 10.1186/1471-2210-10-6.
- 453 Tjørve K.M.C., Tjørve E. (2017) A proposed family of unified models for sigmoidal growth. *Ecological*
454 *Modelling* **359**: 117-127.
- 455 Vattay G. (2020) *Predicting the ultimate outcome of the COVID-19 outbreak in Italy*, preprint published online:
456 arXiv:2003.07912v2 [q-bio.PE]
- 457 Verhulst P.F. (1838) Notice sur la loi que la population suit dans son accroissement. *Corr. Math. Phys.* **10**: 113-
458 121.
- 459 Vidal R.V.V. (1993) *Applied simulated annealing*. Lecture notes in economics and mathematical systems.
460 Berlin: Springer-Verlag 1993.
- 461 WHO (2020) *Coronavirus disease 2019 (COVID-19)*. Situation report No 73, Link: www.who.int (last visit
462 25.07.2020).
- 463 Wu K., Darcet D., Wang Q., Sornette D. (2020) Generalized logistic growth modeling of the COVID-19
464 outbreak in 29 provinces in China and in the rest of the world. *Nonlinear Dynamics*, published online: DOI
465 10.1007/s11071-020-05862-6; see also the preprint DOI 10.1101/2020.03.11.20034363.
- 466 Ziegler M.K., Brunner N., Kühleitner M. (2020) The Markets of Green Cars of Three Countries: Analysis Using
467 Lotka-Volterra and Bertalanffy-Pütter Models. *Journal of Open Innovation: Technology, Market and*
468 *Complexity*, published online: DOI 10.3390/joitmc6030067.
- 469

470 **6. Figures and tables**

471

472 **Figure 1:** Total count of deceased since the begin of the COVID-19 epidemics in Austria (blue dots), and four
473 lines for the BP-model growth-curves with best fit to 100% (black) and 50% (red) of the data, using *SSE* (solid)
474 and *SWSE* (dashed) for calibration.

475



476

477 **Figure 2:** Total count of deceased since the begin of the COVID-19 epidemics in Burkina Faso (blue dots),
478 logistic growth curve (green), best-fit growth curve (black), asymptotic limit (red line), and inflection points (red
479 dots) of the best-fit growth curve (labeled) and the logistic growth curve.

480

481

482 **Table 1** Summary of the data

| Country | Fatalities | | | Confirmed cases | | |
|----------------------------|-------------|---------------------|---------|-----------------|---------------------|-----------|
| | Start | $n_D = \text{days}$ | June 18 | Start | $n_C = \text{days}$ | June 18 |
| Andorra | March 22 | 88 | 52 | March 2 | 108 | 854 |
| Australia: New South Wales | March 4 | 106 | 48 | January 26 | 144 | 3137 |
| Austria | March 12 | 98 | 687 | February 25 | 114 | 17,203 |
| Belgium | March 11 | 99 | 9675 | February 4 | 135 | 60,244 |
| Burkina Faso | March 18 | 92 | 53 | March 10 | 100 | 899 |
| Canada: Alberta | March 20 | 90 | 151 | March 6 | 104 | 7530 |
| Canada: British Columbia | March 9 | 101 | 168 | January 28 | 142 | 2775 |
| Canada: Nova Scotia | April 7 | 72 | 62 | March 16 | 94 | 1061 |
| Canada: Ontario | March 17 | 93 | 2607 | January 26 | 144 | 34,382 |
| Canada: Quebec | March 19 | 91 | 5298 | February 28 | 111 | 54,263 |
| Chad | April 28 | 51 | 74 | March 19 | 91 | 854 |
| China: Hubei | January 22 | 86 | 3222 | January 22 | 148 | 68,135 |
| Croatia | March 19 | 91 | 107 | February 25 | 114 | 2258 |
| Cuba | March 18 | 92 | 84 | March 12 | 98 | 2280 |
| Czechia | March 22 | 88 | 333 | March 1 | 109 | 10,162 |
| Denmark (mainland) | March 14 | 96 | 598 | February 27 | 112 | 12,294 |
| Estonia | March 25 | 85 | 69 | February 27 | 112 | 1977 |
| Finland | March 21 | 89 | 326 | January 29 | 141 | 7117 |
| France (mainland) | February 15 | 124 | 29,512 | January 24 | 146 | 189,906 |
| Germany | March 9 | 101 | 8851 | January 27 | 143 | 188,604 |
| Greece | March 11 | 99 | 187 | February 26 | 113 | 3203 |
| Hungary | March 15 | 95 | 567 | March 4 | 106 | 4078 |
| Ireland | March 11 | 99 | 1710 | February 29 | 110 | 25,341 |
| Israel | March 21 | 89 | 303 | February 21 | 118 | 19,783 |
| Italy | February 21 | 118 | 34,448 | January 31 | 139 | 237,828 |
| Japan | February 13 | 126 | 935 | January 22 | 148 | 17,530 |
| Luxembourg | March 14 | 96 | 110 | February 29 | 110 | 4085 |
| Malaysia | March 17 | 93 | 121 | January 25 | 145 | 8515 |
| Morocco | March 10 | 100 | 213 | March 2 | 108 | 8997 |
| Netherlands (mainland) | March 6 | 104 | 6074 | February 27 | 112 | 49,204 |
| Niger | March 25 | 85 | 67 | March 20 | 90 | 1020 |
| Norway | March 14 | 96 | 243 | February 26 | 113 | 8692 |
| Portugal | March 17 | 93 | 1523 | March 2 | 108 | 37,672 |
| San Marino | March 3 | 107 | 42 | February 27 | 112 | 696 |
| Sierra Leone | April 23 | 56 | 51 | March 31 | 79 | 1249 |
| Slovenia | March 14 | 96 | 109 | March 5 | 105 | 1503 |
| South Korea | February 20 | 119 | 280 | January 22 | 148 | 12,257 |
| Spain | March 3 | 107 | 28,752 | February 1 | 138 | 244,683 |
| Sweden | March 11 | 99 | 5041 | January 31 | 139 | 54,562 |
| Switzerland | March 5 | 105 | 1956 | February 25 | 114 | 31,187 |
| Tajikistan | May 2 | 47 | 51 | April 30 | 49 | 5221 |
| Thailand | March 1 | 109 | 58 | January 22 | 148 | 3135 |
| Tunisia | March 19 | 91 | 50 | March 4 | 106 | 1128 |
| UK (mainland) | March 6 | 104 | 42,153 | January 31 | 139 | 299,251 |
| UK: Channel Island | March 26 | 84 | 48 | March 10 | 100 | 570 |
| UK: Isle of Man | April 1 | 78 | 24 | March 20 | 90 | 336 |
| United Arab Emirates | March 20 | 90 | 295 | January 29 | 141 | 43,364 |
| Uruguay | March 28 | 82 | 24 | March 13 | 97 | 849 |
| USA (mainland) | February 29 | 110 | 117,717 | January 22 | 148 | 2,163,290 |

483 Source: CSSE (2020)

484

485 **Table 2** Best-fit BP-parameters, goodness of fit, and comparison with logistic growth for the cumulative counts
 486 of deceased.

| Country | Parameters | | | | | Goodness of fit | | Logistic | |
|--------------|------------|-------|----------|----------|----------|-----------------|--------|--------------|--------|
| | a | b | c | p | q | SSE | R^2 | ΔAIC | R^2 |
| Andorra | 0.52 | 0.96 | 1.02E-01 | 9.15E-01 | 1.60E-01 | 7.59E+01 | 99.66% | 130.3 | 98.45% |
| AU: NSW | 0.52 | 4.92 | 3.24E-01 | 2.00E-01 | 7.96E-09 | 2.42E+02 | 99.30% | 4.9 | 99.24% |
| Austria | 0.82 | 1.20 | 6.74E-02 | 6.83E-01 | 5.76E-02 | 7.30E+03 | 99.88% | 135.0 | 99.50% |
| Belgium | 0.99 | 1.14 | 1.14E+00 | 6.31E-01 | 1.60E-01 | 1.04E+06 | 99.93% | 168.7 | 99.58% |
| Burkina Faso | 0.21 | 2.94 | 8.83E-02 | 7.15E-01 | 1.36E-05 | 7.42E+01 | 99.73% | 70.6 | 99.39% |
| CAN: Alberta | 0.45 | 2.36 | 8.62E-04 | 5.78E-01 | 3.81E-05 | 5.77E+02 | 99.78% | 77.9 | 99.45% |
| CAN: BC | 0.90 | 1.05 | 5.23E-01 | 5.00E-01 | 2.29E-01 | 7.75E+02 | 99.79% | 103.2 | 99.40% |
| CAN: NS | 0.93 | 1.29 | 3.66E-01 | 3.91E-01 | 8.85E-02 | 7.91E+01 | 99.78% | 43.1 | 99.58% |
| CAN: ONT | 0.85 | 1.20 | 8.15E-02 | 5.38E-01 | 3.38E-02 | 4.78E+04 | 99.95% | 167.7 | 99.65% |
| CAN: QU | 0.80 | 1.19 | 6.70E-02 | 6.68E-01 | 2.24E-02 | 2.22E+05 | 99.93% | 176.2 | 99.52% |
| Chad | 0.63 | 1.01 | 6.78E-01 | 1.27E+00 | 2.49E-01 | 1.53E+02 | 99.43% | 41.3 | 98.61% |
| China: Hubei | 0.99 | 1.34 | 2.27E+01 | 3.52E-01 | 2.09E-02 | 7.22E+04 | 99.94% | 90.8 | 99.81% |
| Croatia | 0.72 | 2.18 | 7.13E-01 | 2.39E-01 | 2.64E-04 | 2.78E+02 | 99.80% | 26.8 | 99.72% |
| Cuba | 1.02 | 1.81 | 7.70E-01 | 1.40E-01 | 4.24E-03 | 6.80E+01 | 99.93% | 9.1 | 99.92% |
| Czechia | 0.59 | 0.99 | 1.54E-01 | 1.39E+00 | 1.35E-01 | 1.96E+03 | 99.81% | 174.4 | 98.59% |
| Denmark | 0.75 | 1.07 | 1.41E-01 | 9.00E-01 | 1.16E-01 | 2.86E+03 | 99.93% | 218.4 | 99.32% |
| Estonia | 0.43 | 1.08 | 5.35E-02 | 9.06E-01 | 5.66E-02 | 1.10E+02 | 99.73% | 143.4 | 98.49% |
| Finland | 1.11 | 1.34 | 2.17E+00 | 2.21E-01 | 5.83E-02 | 3.60E+03 | 99.74% | 21.0 | 99.65% |
| France | 1.08 | 1.22 | 3.89E-01 | 2.88E-01 | 6.84E-02 | 2.36E+07 | 99.88% | 129.7 | 99.63% |
| Germany | 0.90 | 1.17 | 4.78E-01 | 6.51E-01 | 5.60E-02 | 4.90E+05 | 99.96% | 215.2 | 99.63% |
| Greece | 0.60 | 1.02 | 7.29E-02 | 8.27E-01 | 9.12E-02 | 9.59E+02 | 99.75% | 169.7 | 98.53% |
| Hungary | 0.79 | 1.26 | 1.89E-02 | 4.62E-01 | 2.31E-02 | 3.11E+03 | 99.93% | 178.5 | 99.49% |
| Ireland | 1.19 | 1.20 | 1.54E+00 | 2.41E+00 | 2.23E+00 | 7.99E+04 | 99.83% | 29.0 | 99.76% |
| Israel | 0.78 | 1.01 | 2.67E-01 | 9.59E-01 | 2.58E-01 | 1.55E+03 | 99.84% | 153.8 | 99.04% |
| Italy | 0.93 | 1.03 | 5.53E-01 | 1.13E+00 | 3.97E-01 | 1.04E+07 | 99.95% | 281.7 | 99.42% |
| Japan | 1.22 | 1.50 | 1.74E+00 | 6.23E-02 | 9.09E-03 | 1.47E+04 | 99.91% | 7.4 | 99.90% |
| Luxembourg | 0.77 | 1.14 | 2.63E-01 | 5.34E-01 | 9.32E-02 | 3.70E+02 | 99.74% | 104.0 | 99.20% |
| Malaysia | 0.43 | 1.08 | 2.57E-01 | 1.37E+00 | 6.12E-02 | 1.85E+02 | 99.85% | 206.5 | 98.51% |
| Morocco | 0.87 | 1.13 | 6.71E-02 | 5.62E-01 | 1.40E-01 | 2.52E+03 | 99.58% | 102.2 | 98.79% |
| Netherlands | 0.84 | 1.20 | 1.40E-01 | 7.61E-01 | 3.30E-02 | 1.49E+05 | 99.97% | 277.3 | 99.61% |
| Niger | 0.33 | 10.22 | 8.11E-01 | 3.88E-01 | 4.15E-19 | 8.20E+01 | 99.82% | 64.1 | 99.60% |
| Norway | 0.95 | 1.17 | 3.77E-01 | 5.46E-01 | 1.64E-01 | 9.25E+02 | 99.87% | 103.1 | 99.62% |
| Portugal | 0.63 | 0.96 | 8.82E-02 | 1.74E+00 | 1.51E-01 | 3.33E+04 | 99.86% | 199.5 | 98.79% |
| San Marino | 0.68 | 1.26 | 2.51E-02 | 4.84E-01 | 5.54E-02 | 1.15E+02 | 99.44% | 69.9 | 98.89% |
| Sierra Leone | 0.69 | 2.18 | 1.50E+00 | 2.78E-01 | 7.82E-04 | 5.62E+01 | 99.67% | 18.1 | 99.51% |
| Slovenia | 0.83 | 1.24 | 3.55E-02 | 4.45E-01 | 6.49E-02 | 1.74E+02 | 99.89% | 134.7 | 99.53% |
| South Korea | 0.71 | 1.75 | 4.43E+00 | 3.15E-01 | 9.19E-04 | 1.45E+03 | 99.86% | 90.5 | 99.70% |
| Spain | 0.90 | 1.12 | 4.00E-01 | 9.93E-01 | 1.05E-01 | 2.38E+07 | 99.81% | 117.1 | 99.40% |
| Sweden | 0.84 | 1.05 | 3.28E-01 | 7.63E-01 | 1.25E-01 | 3.55E+05 | 99.89% | 177.4 | 99.29% |
| Switzerland | 0.86 | 1.31 | 5.97E-02 | 5.66E-01 | 1.88E-02 | 1.14E+04 | 99.98% | 265.6 | 99.75% |
| Tajikistan | 0.31 | 3.32 | 9.68E-01 | 1.20E+00 | 1.00E-05 | 9.05E+01 | 99.20% | 4.3 | 99.05% |
| Thailand | 1.00 | 1.41 | 5.48E-03 | 3.14E-01 | 5.99E-02 | 1.01E+02 | 99.83% | 103.0 | 99.56% |
| Tunesia | 0.61 | 1.02 | 1.12E-01 | 7.56E-01 | 1.54E-01 | 1.64E+02 | 99.23% | 76.1 | 98.15% |
| UK | 0.95 | 1.02 | 8.53E-01 | 1.31E+00 | 6.22E-01 | 3.20E+07 | 99.88% | 180.1 | 99.27% |
| UK: CI | 1.26 | 1.41 | 1.04E+00 | 3.31E-01 | 1.87E-01 | 1.86E+02 | 99.20% | 20.1 | 98.93% |
| UK: IM | 1.46 | 1.59 | 2.65E-01 | 5.61E-01 | 3.72E-01 | 3.35E+01 | 99.49% | 29.9 | 99.21% |
| UAE | 1.19 | 1.36 | 1.26E+00 | 1.79E-01 | 6.82E-02 | 1.75E+03 | 99.84% | 20.0 | 99.79% |
| Uruguay | 0.00 | 3.16 | 8.68E-01 | 4.68E-01 | 1.97E-05 | 3.78E+01 | 99.06% | 39.3 | 98.40% |
| USA | 0.95 | 1.04 | 7.25E-01 | 9.12E-01 | 3.17E-01 | 1.50E+08 | 99.93% | 220.5 | 99.44% |

487 Notes: Countries the order of Table 1 (names abbreviated); $x.xx\text{E}+/-yy$ means $x.xx \cdot 10^{+/-yy}$ (all numbers rounded
 488 to the two displayed decimals); $\Delta AIC = AIC$ (logistic model) minus AIC (best-fit BP-model).

489 **Table 3** Best-fit BP-parameters, goodness of fit, and comparison with logistic growth for the cumulative counts
 490 of confirmed cases.

| Country | Parameters | | | | | Goodness of fit | | Logistic | |
|--------------|------------|------|----------|----------|----------|-----------------|--------|--------------|--------|
| | a | b | c | p | q | SSE | R^2 | ΔAIC | R^2 |
| Andorra | 0.89 | 1.34 | 2.77E-02 | 5.50E-01 | 2.77E-02 | 6.04E+03 | 99.94% | 156.9 | 99.74% |
| AU: NSW | 1.08 | 1.59 | 1.17E-02 | 2.00E-01 | 3.34E-03 | 2.55E+05 | 99.91% | 33.1 | 99.89% |
| Austria | 0.93 | 1.26 | 3.40E-01 | 6.55E-01 | 2.66E-02 | 2.17E+07 | 99.55% | 68.3 | 99.15% |
| Belgium | 1.09 | 1.18 | 6.34E-01 | 3.06E-01 | 1.14E-01 | 5.37E+07 | 99.94% | 190.5 | 99.73% |
| Burkina Faso | 0.63 | 0.91 | 1.63E-01 | 1.78E+00 | 2.63E-01 | 3.34E+04 | 99.63% | 160.1 | 98.08% |
| CAN: Alberta | 1.26 | 1.69 | 8.03E+01 | 2.59E-02 | 5.70E-04 | 2.52E+06 | 99.71% | -0.2 | 99.70% |
| CAN: BC | 0.92 | 1.31 | 1.84E-02 | 2.57E-01 | 1.17E-02 | 6.60E+05 | 99.60% | 100.2 | 99.17% |
| CAN: NS | 0.64 | 3.08 | 7.63E+00 | 7.35E-01 | 3.08E-08 | 6.30E+03 | 99.96% | 37.9 | 99.93% |
| CAN: ONT | 0.97 | 1.27 | 1.81E-01 | 2.03E-01 | 8.61E-03 | 5.68E+07 | 99.74% | 124.9 | 99.36% |
| CAN: QU | 0.73 | 1.65 | 1.33E-02 | 1.10E+00 | 4.51E-05 | 3.59E+07 | 99.92% | 134.2 | 99.73% |
| Chad | 1.27 | 1.35 | 5.18E-01 | 2.41E-01 | 1.40E-01 | 1.53E+04 | 99.85% | 6.8 | 99.84% |
| China: Hubei | 0.61 | 4.09 | 9.87E+01 | 7.18E+00 | 1.10E-16 | 2.15E+08 | 99.63% | 13.1 | 99.59% |
| Croatia | 0.89 | 1.33 | 2.14E-02 | 4.93E-01 | 1.65E-02 | 5.62E+04 | 99.94% | 186.0 | 99.68% |
| Cuba | 0.9 | 1.08 | 8.07E-01 | 6.93E-01 | 1.73E-01 | 1.87E+05 | 99.71% | 100.7 | 99.16% |
| Czechia | 0.86 | 0.99 | 1.94E+00 | 1.46E+00 | 4.41E-01 | 9.92E+06 | 99.26% | 99.0 | 98.09% |
| Denmark | 0.89 | 1.04 | 1.81E+00 | 9.13E-01 | 2.22E-01 | 2.66E+06 | 99.88% | 150.0 | 99.53% |
| Estonia | 0.87 | 1.14 | 1.99E-01 | 6.77E-01 | 8.82E-02 | 2.03E+05 | 99.64% | 88.6 | 99.19% |
| Finland | 0.93 | 1.36 | 2.92E-02 | 2.40E-01 | 5.23E-03 | 3.93E+05 | 99.97% | 248.3 | 99.79% |
| France | 0.99 | 1.53 | 1.55E-01 | 2.18E-01 | 3.13E-04 | 2.21E+09 | 99.77% | 43.8 | 99.68% |
| Germany | 1.09 | 1.2 | 6.35E-01 | 2.59E-01 | 6.84E-02 | 1.56E+09 | 99.83% | 134.7 | 99.54% |
| Greece | 0.84 | 1.1 | 3.72E-01 | 8.38E-01 | 1.04E-01 | 4.93E+05 | 99.64% | 116.0 | 98.97% |
| Hungary | 0.92 | 1.14 | 5.17E-01 | 5.06E-01 | 8.08E-02 | 1.63E+05 | 99.94% | 177.0 | 99.64% |
| Ireland | 0.79 | 1.85 | 6.94E-03 | 7.85E-01 | 1.70E-05 | 9.19E+06 | 99.92% | 51.0 | 99.87% |
| Israel | 1.02 | 1.24 | 3.59E-01 | 3.69E-01 | 4.32E-02 | 1.04E+07 | 99.84% | 99.8 | 99.60% |
| Italy | 1.02 | 1.13 | 9.21E-01 | 4.45E-01 | 1.14E-01 | 7.31E+08 | 99.94% | 258.6 | 99.63% |
| Japan | 1.26 | 1.75 | 2.00E+01 | 2.07E-02 | 1.76E-04 | 9.37E+06 | 99.88% | 32.2 | 99.85% |
| Luxembourg | 0.93 | 1.21 | 2.19E-01 | 6.78E-01 | 6.66E-02 | 6.63E+05 | 99.74% | 112.6 | 99.26% |
| Malaysia | 0.93 | 1.29 | 1.41E-01 | 2.55E-01 | 9.89E-03 | 1.08E+07 | 99.29% | 84.9 | 98.69% |
| Marocco | 0.99 | 1.06 | 6.67E-01 | 7.45E-01 | 3.93E-01 | 1.03E+06 | 99.91% | 136.7 | 99.67% |
| Netherlands | 0.94 | 1.06 | 8.81E-01 | 9.91E-01 | 2.72E-01 | 3.25E+07 | 99.91% | 178.7 | 99.56% |
| Niger | 0.75 | 0.97 | 2.23E-01 | 1.66E+00 | 3.65E-01 | 1.60E+05 | 98.46% | 70.0 | 96.50% |
| Norway | 0.89 | 1.02 | 7.35E-01 | 1.42E+00 | 4.39E-01 | 1.48E+06 | 99.86% | 178.2 | 99.32% |
| Portugal | 0.89 | 0.9 | 1.26E+00 | 1.31E+01 | 1.18E+01 | 1.19E+08 | 99.33% | 110.2 | 98.07% |
| San Marino | 0.3 | 5.98 | 2.74E-04 | 1.99E+00 | 1.57E-16 | 1.72E+04 | 99.74% | 63.5 | 99.53% |
| Sierra Leone | 0.94 | 1.14 | 3.92E-01 | 3.62E-01 | 8.27E-02 | 2.57E+04 | 99.80% | 48.8 | 99.62% |
| Slovenia | 0.41 | 2.48 | 4.63E-05 | 3.62E+00 | 9.90E-07 | 1.74E+04 | 99.93% | 152.0 | 99.70% |
| South Korea | 0.99 | 1.27 | 2.65E-01 | 3.77E-01 | 2.77E-02 | 4.18E+07 | 98.66% | 46.1 | 98.11% |
| Spain | 1.06 | 1.22 | 4.78E-01 | 2.70E-01 | 3.72E-02 | 2.34E+09 | 99.84% | 139.0 | 99.55% |
| Sweden | 0.88 | 0.98 | 5.27E-01 | 5.91E-01 | 1.83E-01 | 1.55E+08 | 99.59% | 118.4 | 99.01% |
| Switzerland | 0.95 | 1.15 | 3.32E-01 | 8.17E-01 | 1.03E-01 | 6.67E+06 | 99.96% | 240.6 | 99.66% |
| Tajikistan | 1.01 | 1.3 | 6.69E+01 | 3.43E-01 | 2.84E-02 | 2.82E+05 | 99.82% | 26.0 | 99.67% |
| Thailand | 1.1 | 1.45 | 4.51E-02 | 1.66E-01 | 9.99E-03 | 4.07E+05 | 99.85% | 82.7 | 99.74% |
| Tunesia | 0.83 | 1.29 | 4.21E-02 | 6.27E-01 | 2.53E-02 | 3.86E+04 | 99.79% | 116.7 | 99.33% |
| UK | 1.01 | 1.2 | 6.92E-01 | 2.46E-01 | 2.23E-02 | 9.18E+08 | 99.95% | 236.7 | 99.71% |
| UK: CI | 0.88 | 1.3 | 2.12E-02 | 6.37E-01 | 4.47E-02 | 5.81E+03 | 99.87% | 90.9 | 99.66% |
| UK: IM | 1.05 | 1.35 | 4.51E+00 | 3.67E-01 | 6.42E-02 | 2.95E+03 | 99.74% | 19.4 | 99.66% |
| UAE | 0.91 | 1.43 | 7.87E-02 | 2.10E-01 | 7.00E-04 | 1.84E+07 | 99.94% | 111.7 | 99.85% |
| Uruguay | 0.21 | 0.57 | 1.64E+00 | 1.32E+01 | 1.10E+00 | 2.46E+04 | 99.58% | 182.4 | 97.16% |
| USA | 1.01 | 1.08 | 8.09E-01 | 4.51E-01 | 1.61E-01 | 1.77E+11 | 99.79% | 165.4 | 99.33% |

491 Note as for Table 2

492 **Table 4** Further parameters (computed from the best-fit BP-model parameters)

| Country | <i>fatalities</i> | | | <i>confirmed cases</i> | | |
|--------------|-------------------|------------|------------|------------------------|------------|------------|
| | y_{max} | y_{infl} | t_{infl} | y_{max} | y_{infl} | t_{infl} |
| Andorra | 5.25E+01 | 1.30E+01 | 10.64 | 7.63E+02 | 3.07E+02 | 26.90 |
| AU: NSW | 4.81E+01 | 2.89E+01 | 46.72 | 3.06E+03 | 1.43E+03 | 61.35 |
| Austria | 6.70E+02 | 2.46E+02 | 25.79 | 1.64E+04 | 6.52E+03 | 30.02 |
| Belgium | 9.60E+03 | 3.75E+03 | 32.79 | 5.94E+04 | 2.46E+04 | 64.83 |
| Burkina Faso | 5.36E+01 | 2.04E+01 | 19.20 | 9.33E+02 | 2.51E+02 | 20.61 |
| CAN: Alberta | 1.55E+02 | 6.49E+01 | 32.65 | 7.19E+03 | 3.63E+03 | 47.48 |
| CAN: BC | 1.83E+02 | 6.53E+01 | 36.12 | 2.74E+03 | 1.11E+03 | 68.19 |
| CAN: NS | 6.21E+01 | 2.50E+01 | 20.75 | 1.06E+03 | 5.54E+02 | 30.01 |
| CAN: Ontario | 2.73E+03 | 1.02E+03 | 40.65 | 3.74E+04 | 1.52E+04 | 92.65 |
| CAN: Quebec | 6.06E+03 | 2.19E+03 | 45.08 | 5.89E+04 | 2.43E+04 | 57.34 |
| Chad | 7.30E+01 | 2.11E+01 | 8.21 | 8.76E+02 | 4.08E+02 | 56.06 |
| China: Hubei | 3.21E+03 | 1.35E+03 | 22.10 | 6.79E+04 | 3.93E+04 | 20.33 |
| Croatia | 1.06E+02 | 4.96E+01 | 33.97 | 2.25E+03 | 9.02E+02 | 36.00 |
| Cuba | 8.34E+01 | 4.04E+01 | 34.28 | 2.25E+03 | 8.15E+02 | 33.83 |
| Czechia | 3.41E+02 | 9.36E+01 | 16.38 | 9.69E+03 | 3.28E+03 | 30.12 |
| Denmark | 6.05E+02 | 1.99E+02 | 24.17 | 1.25E+04 | 4.43E+03 | 38.38 |
| Estonia | 7.13E+01 | 1.73E+01 | 11.98 | 1.90E+03 | 6.97E+02 | 31.19 |
| Finland | 3.26E+02 | 1.44E+02 | 32.38 | 7.33E+03 | 3.03E+03 | 75.24 |
| France | 2.89E+04 | 1.21E+04 | 54.82 | 1.84E+05 | 8.22E+04 | 73.29 |
| Germany | 8.84E+03 | 3.35E+03 | 35.13 | 1.82E+05 | 7.60E+04 | 65.29 |
| Greece | 1.91E+02 | 5.39E+01 | 21.16 | 3.01E+03 | 1.07E+03 | 30.59 |
| Hungary | 5.84E+02 | 2.16E+02 | 37.93 | 4.17E+03 | 1.57E+03 | 41.86 |
| Ireland | 1.69E+03 | 7.31E+02 | 40.18 | 2.52E+04 | 1.13E+04 | 44.99 |
| Israel | 3.02E+02 | 9.80E+01 | 20.62 | 1.71E+04 | 7.03E+03 | 42.47 |
| Italy | 3.47E+04 | 1.25E+04 | 39.99 | 2.37E+05 | 9.33E+04 | 58.40 |
| Japan | 9.64E+02 | 4.61E+02 | 78.27 | 1.68E+04 | 8.62E+03 | 85.05 |
| Luxembourg | 1.12E+02 | 3.88E+01 | 21.80 | 3.97E+03 | 1.55E+03 | 27.09 |
| Malaysia | 1.19E+02 | 2.89E+01 | 10.35 | 8.35E+03 | 3.36E+03 | 71.40 |
| Marocco | 2.07E+02 | 7.59E+01 | 27.32 | 9.39E+03 | 3.54E+03 | 52.51 |
| Netherlands | 6.12E+03 | 2.27E+03 | 33.78 | 4.82E+04 | 1.77E+04 | 37.80 |
| Niger | 6.56E+01 | 4.64E+01 | 47.06 | 9.77E+02 | 3.03E+02 | 18.25 |
| Norway | 2.38E+02 | 9.25E+01 | 24.48 | 8.51E+03 | 2.98E+03 | 26.79 |
| Portugal | 1.65E+03 | 4.60E+02 | 24.47 | 3.69E+04 | 1.21E+04 | 36.00 |
| San Marino | 4.19E+01 | 1.45E+01 | 17.73 | 6.83E+02 | 4.04E+02 | 48.24 |
| Sierra Leone | 5.15E+01 | 2.38E+01 | 19.90 | 1.61E+03 | 6.13E+02 | 51.80 |
| Slovenia | 1.10E+02 | 4.11E+01 | 26.06 | 1.48E+03 | 6.20E+02 | 21.66 |
| South Korea | 2.74E+02 | 1.15E+02 | 31.52 | 1.11E+04 | 4.56E+03 | 41.59 |
| Spain | 2.77E+04 | 1.02E+04 | 30.55 | 2.37E+05 | 9.86E+04 | 60.11 |
| Sweden | 5.50E+03 | 1.90E+03 | 43.18 | 1.22E+05 | 4.16E+04 | 123.46 |
| Switzerland | 1.94E+03 | 7.61E+02 | 32.08 | 3.08E+04 | 1.18E+04 | 30.27 |
| Tajikistan | 4.86E+01 | 2.21E+01 | 9.25 | 5.36E+03 | 2.25E+03 | 20.71 |
| Thailand | 5.69E+01 | 2.46E+01 | 36.21 | 3.05E+03 | 1.38E+03 | 67.44 |
| Tunesia | 4.87E+01 | 1.39E+01 | 12.79 | 1.08E+03 | 4.13E+02 | 28.44 |
| UK | 4.27E+04 | 1.55E+04 | 41.10 | 3.10E+05 | 1.25E+05 | 80.74 |
| UK: CI | 4.59E+01 | 2.17E+01 | 23.44 | 5.58E+02 | 2.20E+02 | 23.41 |
| UK: IM | 2.37E+01 | 1.23E+01 | 20.75 | 3.34E+02 | 1.44E+02 | 16.91 |
| UAE | 2.91E+02 | 1.33E+02 | 44.36 | 5.81E+04 | 2.44E+04 | 109.48 |
| Uruguay | 2.42E+01 | NA | NA | 9.90E+02 | 6.18E+01 | 3.23 |
| USA | 1.25E+05 | 4.56E+04 | 52.73 | 2.40E+06 | 9.23E+05 | 94.86 |

493 Notes: t_{infl} is the solution of $y(t) = y_{infl}$ (we used only y_{infl} but reported t_{infl} for the sake of completeness); NA
494 means no inflection point; otherwise as in Table 2.

495

496 **Table 5** Further statistics (computed from the previous parameters)

| Country | <i>fatalities</i> | | <i>confirmed cases</i> | | <i>CFR</i> |
|--------------|---------------------|--------------------|------------------------|--------------------|------------|
| | $y_{max}/\max(y_i)$ | y_{infl}/y_{max} | $y_{max}/\max(y_i)$ | y_{infl}/y_{max} | |
| Andorra | 1.01 | 4.03 | 0.89 | 2.48 | 6.9% |
| AU: NSW | 1.00 | 1.67 | 0.98 | 2.13 | 1.6% |
| Austria | 0.98 | 2.72 | 0.95 | 2.51 | 4.1% |
| Belgium | 0.99 | 2.56 | 0.99 | 2.41 | 16.2% |
| Burkina Faso | 1.01 | 2.63 | 1.04 | 3.72 | 5.7% |
| CAN: Alberta | 1.02 | 2.38 | 0.95 | 1.98 | 2.2% |
| CAN: BC | 1.09 | 2.79 | 0.99 | 2.47 | 6.7% |
| CAN: NS | 1.00 | 2.48 | 0.99 | 1.90 | 5.9% |
| CAN: Ontario | 1.05 | 2.68 | 1.09 | 2.46 | 7.3% |
| CAN: Quebec | 1.14 | 2.77 | 1.08 | 2.43 | 10.3% |
| Chad | 0.99 | 3.46 | 1.03 | 2.15 | 8.3% |
| China: Hubei | 0.99 | 2.37 | 1.00 | 1.73 | 4.7% |
| Croatia | 0.99 | 2.14 | 0.99 | 2.49 | 4.7% |
| Cuba | 0.99 | 2.07 | 0.98 | 2.75 | 3.7% |
| Czechia | 1.03 | 3.65 | 0.95 | 2.95 | 3.5% |
| Denmark | 1.01 | 3.04 | 1.02 | 2.82 | 4.8% |
| Estonia | 1.03 | 4.12 | 0.96 | 2.72 | 3.8% |
| Finland | 1.00 | 2.27 | 1.03 | 2.42 | 4.4% |
| France | 0.98 | 2.39 | 0.97 | 2.24 | 15.7% |
| Germany | 1.00 | 2.64 | 0.97 | 2.40 | 4.9% |
| Greece | 1.02 | 3.54 | 0.94 | 2.82 | 6.3% |
| Hungary | 1.03 | 2.70 | 1.02 | 2.65 | 14.0% |
| Ireland | 0.99 | 2.31 | 0.99 | 2.23 | 6.7% |
| Israel | 1.00 | 3.08 | 0.86 | 2.43 | 1.8% |
| Italy | 1.01 | 2.78 | 1.00 | 2.54 | 14.7% |
| Japan | 1.03 | 2.09 | 0.96 | 1.96 | 5.7% |
| Luxembourg | 1.02 | 2.89 | 0.97 | 2.56 | 2.8% |
| Malaysia | 0.98 | 4.12 | 0.98 | 2.48 | 1.4% |
| Marocco | 0.97 | 2.73 | 1.04 | 2.65 | 2.2% |
| Netherlands | 1.01 | 2.69 | 0.98 | 2.72 | 12.7% |
| Niger | 0.98 | 1.41 | 0.96 | 3.22 | 6.7% |
| Norway | 0.98 | 2.58 | 0.98 | 2.85 | 2.8% |
| Portugal | 1.08 | 3.58 | 0.98 | 3.06 | 4.5% |
| San Marino | 1.00 | 2.90 | 0.98 | 1.69 | 6.1% |
| Sierra Leone | 1.01 | 2.16 | 1.29 | 2.62 | 3.2% |
| Slovenia | 1.00 | 2.66 | 0.98 | 2.39 | 7.4% |
| South Korea | 0.98 | 2.38 | 0.91 | 2.43 | 2.5% |
| Spain | 0.96 | 2.70 | 0.97 | 2.41 | 11.7% |
| Sweden | 1.09 | 2.89 | 2.24 | 2.93 | 4.5% |
| Switzerland | 0.99 | 2.55 | 0.99 | 2.60 | 6.3% |
| Tajikistan | 0.95 | 2.20 | 1.03 | 2.39 | 0.9% |
| Thailand | 0.98 | 2.31 | 0.97 | 2.20 | 1.9% |
| Tunesia | 0.97 | 3.50 | 0.96 | 2.61 | 4.5% |
| UK | 1.01 | 2.76 | 1.03 | 2.48 | 13.8% |
| UK: CI | 0.96 | 2.12 | 0.98 | 2.53 | 8.2% |
| UK: IM | 0.99 | 1.93 | 0.99 | 2.31 | 7.1% |
| UAE | 0.99 | 2.19 | 1.34 | 2.39 | 0.5% |
| Uruguay | 1.01 | NA | 1.17 | 16.02 | 2.4% |
| USA | 1.06 | 2.73 | 1.11 | 2.60 | 5.2% |

497 Notes: $\max(y_i)$ are the June 18 counts of Table 1; *CFR* is the case fatality rate and lower/upper are estimates for
498 the minimal/maximal rates of other “good fitting” models (based on a simulation); otherwise as in Table 4.

The authors declare no competing interests and there did not arise ethical issues, as we used ethically unproblematic data from open sources. Links to these data are provided in the paper.

Journal Pre-proof